

**Accurate and simple method for quantification of hepatic fat content using magnetic resonance imaging: a prospective study in biopsy-proven nonalcoholic fatty liver disease**

Tomoko Hatta,<sup>1</sup> Yasunari Fujinaga,<sup>1</sup> Masumi Kadoya,<sup>1</sup> Hitoshi Ueda,<sup>2</sup> Hiroaki Murayama,<sup>2</sup> Masahiro Kurozumi,<sup>1</sup> Kazuhiko Ueda,<sup>1</sup> Michiharu Komatsu,<sup>3</sup> Tadanobu Nagaya,<sup>3</sup> Satoru Joshita,<sup>3</sup> Ryo Kodama,<sup>3</sup> Eiji Tanaka,<sup>3</sup> Tsuyoshi Uehara,<sup>4</sup> Kenji Sano<sup>4</sup>, Naoki Tanaka<sup>3,5</sup>

1. Department of Radiology, Shinshu University School of Medicine, Matsumoto, Japan
2. Section of Radiology, Shinshu University Hospital, Matsumoto, Japan
3. Department of Gastroenterology, Shinshu University School of Medicine, Matsumoto, Japan
4. Section of Laboratory Medicine, Shinshu University Hospital, Matsumoto, Japan
5. Department of Metabolic Regulation, Shinshu University Graduate School of Medicine, Matsumoto, Japan.

**Correspondence to:** Masumi Kadoya, MD, PhD, Department of Radiology, Shinshu University School of Medicine, Asahi 3-1-1, Matsumoto, 390-8621, Japan.

**E-mail:** [kadoyam@shinshu-u.ac.jp](mailto:kadoyam@shinshu-u.ac.jp)

**Short title:** Quantification of hepatic fat using MRI

**Keywords:** Fatty liver; Magnetic resonance imaging; Water-oil phantom; Liver biopsy

## **Abstract**

**Background:** To assess the degree of hepatic fat content, simple and noninvasive methods with high objectivity and reproducibility are required. Magnetic resonance imaging (MRI) is one such candidate, although its accuracy remains unclear. We aimed to validate an MRI method for quantifying hepatic fat content by calibrating MRI reading with a phantom and comparing MRI measurements in human subjects with estimates of liver fat content in liver biopsy specimens.

**Methods:** The MRI method is performed by the combination of MRI calibration using a phantom and double-echo chemical shift gradient-echo sequence (double-echo fast low-angle shot sequence) that has been widely used on a 1.5-T scanner. Liver fat content in patients with nonalcoholic fatty liver disease (NAFLD, n = 26) was derived from a calibration curve generated by scanning the phantom. Liver fat was also estimated by optical image analysis. The correlation between the MRI measurements and liver histology findings was examined prospectively.

**Results:** Magnetic resonance imaging measurements showed a strong correlation with liver fat content estimated from the results of light microscopic examination (correlation coefficient 0.91,  $P < 0.001$ ) regardless of the degree of hepatic steatosis. Moreover, the severity of lobular inflammation or fibrosis did not influence the MRI measurements.

**Conclusion:** This MRI method is simple and noninvasive, has an excellent ability to quantify hepatic fat content even in NAFLD patients with mild steatosis or advanced fibrosis, and can be easily performed without special devices.

## **Introduction**

Recently, the prevalence of nonalcoholic fatty liver disease (NAFLD) has been increasing throughout the world, with NAFLD considered to be a common cause of chronic liver disease in Western countries, as well as in Japan.<sup>1-6</sup> NAFLD exhibits a wide spectrum ranging from simple steatosis to nonalcoholic steatohepatitis (NASH). NASH is a histological condition characterized by fatty infiltration of the liver, hepatocyte ballooning, lobular inflammation, and perisinusoidal fibrosis,<sup>1-3,5,7,8</sup> and the degree of hepatic steatosis is one of the essential components used to evaluate the histological activity of NASH. Thus, it is important to correctly know the degree of fatty infiltration when we assess the therapeutic effect in NAFLD/NASH patients.

Liver biopsy is currently considered as the gold standard for the assessment of NAFLD/NASH, but its invasive nature makes it not justify repeated biopsies to study the natural history of NAFLD or the response to therapeutic interventions for NAFLD. Furthermore, the large numbers of NAFLD patients means that the routine use of liver biopsy in this context is unrealistic. Additionally, liver biopsy is subject to the risk of sampling error, especially in patients with advanced NASH, which shows severe fibrosis and heterogeneously distributed fatty infiltration in the liver. Hence, a simple, accurate, and noninvasive method to assess temporal changes in fatty infiltration of the liver is strongly desired.

Radiological imaging studies such as ultrasonography (US), computed tomography (CT) and magnetic resonance imaging (MRI) have so far been employed as noninvasive methods for assessing hepatic steatosis.<sup>2,3,9-11</sup> US is a simple and common examination modality, but is subject to technician-related bias. CT is able to assess fatty deposition objectively, but exposes the patient to radiation. In addition, according to the study of

Saadeh et al,<sup>11</sup> CT and US have a low sensitivity, of <33%, in the case of fatty infiltration, and these modalities may miss some cases of mild steatosis. On the other hand, MRI has better objectivity and has the advantage of no radiation exposure. Moreover, MRI has a greater ability to differentiate tissue characterization than US and CT, thereby facilitating the detection of slighter degrees of fatty infiltration of the liver.<sup>11-16</sup>

Of all MRI techniques, double-echo chemical shift gradient-echo technique is the most sensitive to detect fat,<sup>14,15,17-23</sup> and many studies have used this technique to evaluate hepatic steatosis. However, these studies lacked a basic experiment using a phantom or quantitative evaluation in histopathological assessment of hepatic fat content, or prospective study design, and were semi-quantitative in nature because of inclusion of a classification of the fat content rate.

Against this background, we formulated a simple and accurate MRI method to quantify the degree of fatty infiltration of the liver using double-echo chemical shift gradient-echo sequence [double-echo fast low-angle shot (FLASH) sequence] on a 1.5-T scanner. This method does not require specialized software or hardware. For this investigation, we designed a 3-step process comprising (1) a basic experiment using phantom, (2) a prospective clinical study using liver biopsy specimens and (3) quantitative histopathological estimation of liver fat by optical image analysis using commercial software. Furthermore, we sought to demonstrate the accuracy and usefulness of this convenient method for quantifying liver fat content by comparing MRI measurements with liver fat content calculated by light microscopic findings in biopsy-proven NAFLD patients.

## **Methods**

### ***Theory***

The principle of diagnosing hepatic steatosis by double-echo chemical shift gradient-echo MRI is based on the utilization of the difference in the precessional frequency between water and fat protons.<sup>12-15</sup> At 1.5-T, fat protons precess in the *xy*-plane at a rotational velocity 225 Hz slower than that of water protons. This translates into one less rotation every 4.4 ms or one-half rotation differences every 2.2 ms. In chemical shift imaging, the difference in resonance frequency of water and fat is exploited to create “in-phase (IP)” and “opposed-phase (OP)” images (Fig. 1). By varying the time between excitation and signal acquisition in gradient echo imaging, the magnetic moments of fat and water can be manipulated to lie in either parallel (IP) or anti-parallel (OP) positions. In voxels (volume elements of an MR image) containing a mixture of fat and water, magnetic moment cancellation occurs for OP (but not for IP) images. Thus, a measurable loss of signal in an OP image relative to that of an IP image indicates the presence of voxels containing both water and fat.

### ***MRI Technique***

All MR scans were performed with one of two 1.5-T scanners (Symphony or Avanto; Siemens, Erlangen, Germany) with a body-array coil. All software used for the study was included in scanners as standard equipment.

An *in vitro* phantom (water-oil phantom) was used to establish a calibration of fat determination based on the double-echo FLASH technique. An *in vivo* study, using this phantom calibration and the same MRI methodology, was then performed to assess liver fat content in patients.

For the phantom study, double-echo FLASH imaging was performed with a repetition time (TR) of 100 ms, double echo times (TEs) of 2.2 ms for OP and 4.4 ms for IP, flip angle of 80° (Avanto) and 90° (Symphony), slice thickness of 5 mm, 32×32 cm field of view and 320×320 matrix, with use of a body-array coil.

For the clinical study, MR scans were performed with TR of 145 ms (Avanto) and 80-103 ms (Symphony), TEs of 2.2 and 4.4 ms (both Avanto and Symphony), and a flip angle of 80° (Avanto) and 90° (Symphony), 256×(256-192) matrix and the field of view was increased to 26×26cm – 34×34cm depending on the patient size, with a body-array coil. Transverse images were obtained with a 6 mm slice thickness and a 2 mm inter-slice gap.

### ***Study 1 (Phantom Study)***

We used a phantom model that consisted of a test tube filled with water (physiological saline; Otsuka, Tokyo, Japan) and mineral oil (Johnson's baby; Johnson & Johnson, New Brunswick, NJ, USA). The oil was layered on water, which provided an oil-water interface in which to test various fractions of fat to water (Fig. 2). Imaging of the water-oil phantom was repeated with the phantom in a horizontal position. Six sections that were each composed of 5-mm-thick slices were obtained parallel to the water-oil interface by using the double-echo FLASH sequence. The location of the six sections was then processed in increments of 0.5mm at a time to create a stepwise quantifiable transition across the water-oil interface [i.e., from 0% to 50% oil (in increments of 10%) in each slice, respectively].

Data were analyzed using a region of interest (ROI) of 9.8cm<sup>2</sup> on each IP and OP image. Data acquisition was repeated three times, and the average value of three

measurements was appropriated to a calibration reference for liver fat quantification.

Quantitative measurement of signal intensity (SI) changes between IP and OP images was calculated as follows: the signal intensity (SI) ratio =  $SI_{op}/SI_{in}$ , where  $SI_{in}$  is SI measured on IP images and  $SI_{op}$  is SI measured on OP images. The SI ratio was plotted against known fat percentages and the data were fit to a polynomial function using Microsoft Office Excel 2003 (Microsoft corporation, Redmond, WA, USA), which served as a calibration reference for hepatic fat quantification.

### ***Study 2 (Clinical Study)***

The study protocol was approved by the Committee for Medical Ethics of Shinshu University School of Medicine (the approved ID number is 927). Informed consent was obtained from all patients.

For validation analysis, 26 consecutive patients with NAFLD were enrolled (12 men, 14 women; mean age, 44.7 years; range, 20-80 years). The possibility of NAFLD was considered according to the following criteria: (1) the presence of hepatorenal contrast and increased hepatic echogenicity on abdominal US; (2) no consumption of alcohol; (3) the absence of other causes of liver dysfunction such as chronic viral hepatitis, drug-induced liver injury, autoimmune liver disease, primary biliary cirrhosis, primary sclerosing cholangitis, Wilson's disease, hereditary hemochromatosis and  $\alpha$ 1-antitrypsin deficiency. The diagnosis of NAFLD/NASH was confirmed by US-guided percutaneous liver biopsy. The histological activity and severity of NAFLD were assessed by an independent pathologist (KS) in a blinded fashion according to the scoring system proposed by Kleiner et al.<sup>5</sup> NASH is defined as the presence of macrovesicular steatosis (> 5% of hepatocyte affected), hepatocyte ballooning, and lobular inflammation.

Body height and weight were measured before liver biopsy in the fasting state, and any underlying diseases, medical interventions, and past medical history were also recorded. The presence of obesity was defined as having a body mass index (BMI) of more than 25 kg/m<sup>2</sup>, based on criteria released by the Japan Society for the Study of Obesity.<sup>24</sup> Patients were considered hypertensive if their systolic/diastolic pressure was greater than 140/90 mmHg, or if they were taking anti-hypertensive drugs. Patients were considered to have hyperlipidemia if their fasting serum levels of cholesterol and triglycerides were equal to or higher than 220 mg/dL and 150 mg/dL, respectively, or if they were taking lipid-lowering drugs.<sup>25-27</sup> All laboratory data were obtained in a fasting state before liver biopsy.

All patients had an MRI scan immediately before US-guided percutaneous liver biopsy. The MR images were analyzed with a commercial software package, EV client (PSP Corporation, Tokyo, Japan). Using this software, we can set out an ROI in the same location and the same area for each IP and OP image pair (Fig. 3). For each case, hepatic SI was measured by three oval ROIs that were selected in the anterior segment of the right lobe of the liver in three slices in an effort to include the biopsy area, and were placed in the liver parenchyma to exclude contamination from blood vessels, motion artifacts, or partial volume effects. The area of these ROIs varied between 269-1501 mm<sup>2</sup> because the ROIs were set apart from large vessels.

Mean pixel SI levels for each ROI were used to calculate the SI ratio. The SI ratio within the ROI was entered into the polynomial function representing the calibration curve and a measurement of hepatic fat content was obtained by solving the equation.

### ***Histopathological Analysis***

Liver biopsy specimens were obtained from segment 5 or 8 using 14-G needles and immediately fixed in 10% neutral formalin. Sections were cut at 4- $\mu$ m thickness and stained using hematoxylin and eosin and Azan-Mallory methods.

Digital images of hematoxylin and eosin-stained liver biopsy sections were converted into a gray scale, and evaluated to maximize the contrast between fat droplets and hepatocytes, connective tissue, and vascular or biliary structures (Fig. 4). PhotoShop 7.0 (Adobe, San Jose, CA, USA) was used to inspect the digital images and to count the total number of pixels corresponding to fat globules. The total number of pixels corresponding to fat globules was divided by the total number of pixels in an entire field to calculate the area fraction representing fat. Twenty microscopic fields ( $\times 400$ ) of each case were selected at random, and the fat fraction of each field was measured. The average of the measurements for all 20 fields was used as the representative liver fat content of each patient.

In addition, hepatic iron deposition that was identified with Perls' Prussian blue stain was evaluated in all biopsy specimens. The severity of iron deposition was classified into five grades according to a previous report<sup>28</sup>, as follows: grade 0, granules were absent or barely discernible at  $\times 400$  magnification; grade 1, granules were barely discernible at  $\times 250$  magnification or were easily confirmed at  $\times 400$  magnification; grade 2, discrete granules were visible at  $\times 100$  magnification; grade 3, discrete granules were visible at  $\times 25$  magnification; and grade 4, masses were visible at  $\times 10$  magnification or with visual observation.

### ***Statistical Analysis***

Statistical analysis was performed with Microsoft Excel 2003 (Microsoft, Redmond,

WA, USA). Linear regression analysis and the Pearson's correlation coefficient were used to examine the association between MRI measurements and optical image analysis results. Data were expressed as mean  $\pm$  standard error (SE). In addition, we analyzed the effects of significant fibrosis (stage 2-4) or lobular inflammation (score 2 and 3) on the correlation between the MRI measurements and optical image analysis results. A value of  $P < 0.05$  was considered to indicate a statistically significant difference.

## **Results**

### ***Study 1 (Phantom study)***

The fat fractions versus measured SI ratio with the phantom are plotted in Fig. 5. The association between mean SI ratio and fat content was well approximated by a cubic polynomial function, independently of the degree of fat fractions. This result suggests that substituting the SI ratio obtained from this MRI method can reflect hepatic actual fat content.

### ***Study 2 (Clinical study)***

To examine whether this system can apply to measurement of hepatic fat content in vivo, MRI measurements were performed in 26 NAFLD patients just before liver biopsy and compared with histological findings. The baseline characteristics of the patients and the liver biopsy findings are summarized in Table 1 and 2, respectively. Twenty-one patients (81%) had obesity, and 15 (58%) were diagnosed as having NASH.

The results of optical image analysis and MRI determined percentage of fat for all patients was  $21.5 \pm 8.6$  and  $22.9 \pm 9.5\%$ , respectively. MRI measurements were significantly correlated with estimates of liver fat content made by optical image analysis (Fig. 6,  $r = 0.91$ ,  $P < 0.001$ ). In addition, even in patients with mild steatosis (5-33% of hepatocytes affected), the MRI measurements correlated well with the estimates ( $r = 0.91$ ,  $P < 0.001$ ). The error between MRI measurements and optical image analysis in patients with fatty deposit less or equal 33% and more than 33% are  $3.2 \pm 2.5\%$  and  $3.9 \pm 1.0\%$ , respectively. As shown in Fig. 7 and 8, such a favorable correlation was maintained even in patients with significant fibrosis (stage 2-4,  $n = 6$ ) or active lobular inflammation (score 2 and 3,  $n = 13$ ) ( $r = 0.93$  and  $r = 0.94$ ,  $P < 0.001$ ,

respectively).

NAFLD, especially NASH, is reported to be sometimes associated with increased iron deposition in the liver, and severe iron deposition may affect MR SI. Liver iron deposition was detected in 3 patients, and all the patients met the criteria for grade 1. The error between the MRI measurements and the optical image analysis in patients without and with iron deposit are  $3.3 \pm 2.5\%$  and  $2.4 \pm 2.1\%$ , respectively.

## **Discussion**

In the present study, hepatic fat content estimated by MRI on the basis of MR theory, was significantly correlated with hepatic fat content calculated by histological evaluation. Furthermore, even in patients with mild steatosis or significant fibrosis, quantification using this method tended to show a good correlation. These results demonstrate that the combination of a detailed MRI calibration using a water-oil phantom and double-echo FLASH sequence has accuracy comparable to that of estimates from liver histology in quantifying hepatic fat content. As far as we know, this is the first prospective study to validate the accuracy and utility of this convenient MR method for quantifying liver fat content.

MR approaches for quantification of hepatic fat content are divided into two categories: MRI and MR spectroscopy (MRS). Investigating the chemical shift by application of spin echo pulse sequences, the so-called Dixon method,<sup>12</sup> has already shown significant correlations for the quantitative assessment of hepatic fat content. However, this MR technique was limited by an increased scanning time, which had to rely on the patient's ability to hold their breath. MRS has also been validated as a reliable test for quantifying liver fat,<sup>29,30</sup> but it relies on a single measurement from a predetermined ROI. Thus, it does not provide an assessment of the whole liver, or retrospective selection of an ROI.

We selected chemical shift MRI technique, i.e. the double-echo FLASH technique, in this study, because this technique has the following advantages: 1) it ensures that both IP and OP images are obtained from the same anatomic position, regardless of the patient's ability to hold their breath, so that it eliminates the problem of slice misintegration that can occur when two acquisitions are performed, 2) all of the

parameters except the TE are similar between in-phase and opposed-phase, and therefore the differences in MR SI between the two images are based only on parallel, respectively opposed water and fat protons. The 2-point and 3-point Dixon method should be compared with double-echo FLASH MRI, but the latter method is superior to the former in that the 3-point Dixon method was less affected by iron than the 2-point one.<sup>31,32</sup> Though the 3-point Dixon method has not become widely used, the fat-quantification method using phantom-calibration in this study is directly applicable to it.

The remarkable advantage of our method is that there is no need for special hardware and software. Therefore, at any institution having a 1.5-T MRI scanner, the quantification of hepatic steatosis based on this method can be performed, although the preparatory step that the collection of phantom data of each MRI scanner is needed for the evaluation of patient data. This preparation step appears to be difficult, but is actually simple and easy when a skilled MRI technician cooperates with the radiologist because the phantom study can be performed without any special material and software. Admittedly, it takes some time to prepare this step. However, this preparation is the only indispensable step for accurate quantification. Recent studies have demonstrated that a technique using selective saturation with a 3.0-T MRI scanner quantified liver fat content relatively well,<sup>21,33</sup> but 3.0-T MRI scanners are not commonly available at present.

Many previous studies using MRI were not calibrated through comparison with a phantom, and less reproducibility was obtained with the technique described here.<sup>19-23</sup> In contrast with these previous studies, we compared MRI findings with optical image analysis data using software and found that measurements from the two modalities were

linearly related and highly correlated. In most previous studies to compare MRI measurements with actual hepatic fat contents, histopathological evaluation was limited to subjective semiquantitative grading by pathologists. Therefore, if the grade of fat deposition after therapy was the same as before, this conventional method could not reveal small changes in fat deposition. This problem, however, could be resolved by our methods.

In our MRI method, there is a possibility to underestimate the degree of fat deposition in the patients having severe steatosis. Because the OP images accurately reflect the differences in water and fat signals, it is impossible to identify whether fat or water is the dominant signal. For example, the SI on OP images in the condition with “water: fat = 40: 60” and that in the condition with “water: fat = 60: 40” are equal. Therefore, the combination with other methods (e.g., MRS) or imaging modalities (e.g., CT) is needed to evaluate hepatic fat content accurately if severe steatosis is suspected.

Gradient-echo sequences have high sensitivity to local magnetic field inhomogeneity caused by iron deposition, and iron deposition in the liver could mask the presence of fat on opposed-phase MR imaging. Westphalen et al<sup>34</sup> showed that MRI evaluation was significantly correlated with histopathologically determined liver fat percentage in patients without iron deposition, while no such correlation was found in patients with iron deposition. It is necessary to consider the influence of iron concentration on the application of our method to liver fat evaluation depending on objective disease (e.g., hepatitis C). The 3-point Dixon method has the advantage that there is no need to take into account the influence of iron deposits, but this sequence is inferior to our method with respect to general versatility because this sequence is cannot be performed without using special software at the present time.

To follow the clinical course and therapeutic response in NAFLD/NASH patients, appropriate means to quantitatively evaluate hepatic fat content are needed. Quantification of hepatic fat content using MRI was comparable to that based on histological evaluation even in humans with mild fatty deposition in the liver. Additionally, the present method is noninvasive and can be performed easily and repeatedly. Therefore it may be applicable to not only routine follow-up and evaluation of therapeutic response for NAFLD/NASH patients, but also annual health check-up in healthy individuals and preoperative examination of candidate donors of living-related liver transplantation.

Clinically, accurate and noninvasive methods to distinguish NASH from NAFLD are desired. Recently, Iijima et al<sup>35</sup> reported that the contrast enhanced US (using Levovist) is a useful screening examination of NASH. In their study, the differential finding between NASH and NAFLD in delayed phase contrast enhancement was attributed to a change in the sinusoidal endothelial system. If a new MRI contrast agent is developed that reflects pathological changes such as the perisinusoidal fibrosis seen in NASH, both the accurate quantification of hepatic fat content and the diagnosis of NASH might be obtained with a single MRI examination.

In conclusion, the double-echo FLASH technique on a 1.5-T MRI scanner provides a simple, accurate and noninvasive means to quantify liver fat content. Although this is a prospective validation study, the number of patients enrolled was small and mild steatosis was the predominant condition. Further studies are needed to confirm the clinical usefulness of this convenient method.

## References

1. Falck-Ytter Y, Younossi ZM, Marchesini G, McCullough AJ. Clinical features and natural history of nonalcoholic steatosis syndromes. *Semin Liver Dis* 2001; 21: 17-26.
2. Clark JM, Brancati FL, Diehl AM. Nonalcoholic fatty liver disease. *Gastroenterology* 2002; 122: 1649-57.
3. Sanyal AJ. AGA Technical Review on Nonalcoholic fatty liver disease. *Gastroenterology* 2002; 123: 1705-25.
4. Clark JM, Brancati FL, Diehl AM. The prevalence and etiology of elevated aminotransferase levels in the United States. *Am J Gastroenterol* 2003; 98: 960-7.
5. Kleiner DE, Brunt EM, Van Natta M, Behling C, Contos MJ, Cummings OW, et al. Design and validation of a histological scoring system for nonalcoholic fatty liver disease. *Hepatology* 2005; 41: 1313-21.
6. Nonomura A, Enomoto Y, Takeda M, Tamura T, Kasai T, Yoshikawa T, et al. Clinical and pathological features of non-alcoholic steatohepatitis. *Hepatol Res* 2005; 33: 116-21.
7. Matteoni CA, Younossi ZM, Gramlich T, Boparai N, Liu YC, McCullough AJ. Nonalcoholic Fatty Liver Disease: a spectrum of clinical and pathological severity. *Gastroenterology* 1999; 116: 1413-9.
8. Brunt EM, Janney CG, Di Bisceglie AM, Neuschwander-Tetri BA, Bacon BR. Nonalcoholic steatohepatitis: a proposal for grading and staging the histological lesions. *Am J Gastroenterol* 1999; 94: 2467-74.
9. Siegelman ES, Rosen MA. Imaging of hepatic steatosis. *Semin Liver Dis* 2001; 21: 71-80.

10. Ricci C, Longo R, Gioulis E, Bosco M, Pollesello P, Masutti F, et al. Noninvasive in vivo quantitative assessment of fat content in human liver. *J Hepatol* 1997; 27: 108-13.
11. Saadeh S, Younossi ZM, Remer EM, Gramlich T, Ong JP, Hurley M, et al. The utility of radiological imaging in nonalcoholic fatty liver disease. *Gastroenterology* 2002; 123: 745-50.
12. Dixon WT. Simple proton spectroscopic imaging. *Radiology* 1984; 153: 189-94.
13. Lee JK, Dixon WT, Ling D, Levitt RG, Murphy WA. Fatty infiltration of the liver: demonstration by proton spectroscopic imaging. *Radiology* 1984; 153: 195-201.
14. Fishbein MH, Gardner KG, Potter CJ, Schmalbrock P, Smith MA. Introduction of fast MR imaging in the assessment of hepatic steatosis. *Magn Reson Imaging* 1997; 15: 287-93.
15. Delfaut EM, Beltran J, Johnson G, Rousseau J, Marchandise X, Cotten A. Fat suppression in MR imaging: techniques and pitfalls. *Radiographics* 1999; 19: 373-82.
16. Mitchell DG, Kim I, Chang TS, Vinitiski S, Consigny PM, Saponaro SA, et al. Chemical shift phase-difference and suppression magnetic resonance imaging techniques in animals, phantoms, and humans. *Invest Radiol* 1991; 26: 1041-52.
17. Levenson H, Greensite F, Hoefs J, Friloux L, Applegate G, Silva E, et al. Fatty infiltration of the liver: quantification with phase contrast MR imaging at 1.5 T vs biopsy. *Am J Roentogenol* 1991; 156: 307-12.
18. Namimoto T, Yamashita Y, Mitsuzaki K, Nakayama Y, Makita O, Kadota M, et al. Adrenal masses: quantification of fat content with double-echo chemical shift in-phase and opposed-phase FLASH MR images for differentiation of adrenal

- adenomas. *Radiology* 2001; 218: 642-6.
19. Rinella ME, McCarthy R, Thakrar K, Finn JP, Rao SM, Koffron AJ, et al. Dual-echo, chemical shift gradient-echo magnetic resonance imaging to quantify hepatic steatosis: implications for living liver donation. *Liver Transpl* 2003; 9: 851-6.
  20. Pilleul F, Chave G, Dumortier J, Scoazec JY, Valette PJ. Fatty infiltration of the liver: detection and grading using dual T1 gradient echo sequences on clinical MR system. *Gastroenterol Clin Biol* 2005; 29: 1143-7.
  21. Schuchmann S, Weigel C, Albrecht L, Kirsch M, Lemke A, Lorenz G, et al. Non-invasive quantification of hepatic fat fraction by fast 1.0, 1.5, 3.0 T MR imaging. *Eur J Radiol* 2007; 62: 416-22.
  22. Hussain HK, Chenevert TL, Londy FJ, Gulani V, Swanson SD, McKenna B, et al. Hepatic fat fraction: MR imaging for quantitative measurement and display---early experience. *Radiology* 2005; 237: 1048-55.
  23. Kim SH, Lee JM, Han JK, Lee JY, Lee KH, Han CJ, et al. Hepatic macrosteatosis: predicting appropriateness of liver donation by using MR imaging---correlation with histopathologic findings. *Radiology* 2006; 240: 116-29.
  24. The Examination Committee of Criteria for 'Obesity Diseases' in Japan, Japan Society for the Study of Obesity. New Criteria for 'Obesity Disease' in Japan. *Circ J* 2002; 66: 987-92.
  25. Tanaka N, Ichijo T, Okiyama W, Mutou H, Misawa N, Matsumoto A, et al. Laparoscopic findings in patients with nonalcoholic steatohepatitis. *Liver Int* 2006; 26: 32-8.
  26. Tanaka N, Tanaka E, Sheena Y, Komatsu M, Okiyama W, Misawa N, et al. Useful parameters for distinguishing nonalcoholic steatohepatitis with mild steatosis from

- cryptogenic chronic hepatitis in the Japanese population. *Liver Int* 2006; 26: 956-63.
27. Tanaka N, Sano K, Horiuchi A, Tanaka E, Kiyosawa K, Aoyama T. Highly-purified eicosapentaenoic acid treatment improves nonalcoholic steatohepatitis. *J Clin Gastroenterol* 2008; 42: 413-8.
  28. Searle JW, Kerr JFR, Halliday JW, Powell LW. Iron storage disease. In: MacSween RNM, Anthony PP, Scheuer PJ, editors. *Pathology of the liver*. 2nd ed. Edinburgh: Churchill Livingstone; 1987
  29. Szczepaniak LS, Babcock EE, Schick FD, Garg A, Dobbins RL, Burns T, et al. Measurement of intracellular triglyceride stores by <sup>1</sup>H spectroscopy and validation in vivo. *Am J Physiol* 1999; 276: E977-89.
  30. Longo R, Pllesello P, Ricci C, Masutti F, Kvam BJ, Bercich L, et al. Proton MR spectroscopy in quantitative in vivo determination of fat content in human steatosis. *J Magn Reson Imaging* 1995; 5: 281-5.
  31. Lodes CC, Felmlee JP, Ehman RL, Sehgal CM, Greenleaf JF, Glover GH, et al. Proton MR chemical shift imaging using double and triple phase contrast acquisition methods. *J Comput Assist Tomogr.* 1989;13:855–61.
  32. Szumowski J, Coshow WR, Li F, Quinn SF. Phase unwrapping in the three-point Dixon method for fat suppression MR imaging. *Radiology.* 1994;192:555–61.
  33. Cotler SJ, Guzman G, Layden-Almer J, Mazzone T, Layden TJ, Zhou XJ. Measurement of liver fat content using selective saturation at 3.0T. *J Magn Reson Imaging* 2007; 25: 743-8.
  34. Westphalen AC, Qayyum A, Yeh BM, Merriman RB, Lee JA, Lamba A, et al. Liver fat: effect of hepatic iron deposit on evaluation with opposed-phase MR imaging. *Radiology* 2007; 242: 450-5.

35. Iijima H, Moriyasu F, Tsuchiya K, Suzuki S, Yoshida M, Shimizu M, et al. Decrease in accumulation of ultrasound contrast microbubbles in non-alcoholic steatohepatitis. *Hepatol Res* 2007; 37: 722-30.

Table 1. Baseline characteristics of the patients

Parameter	Mean $\pm$ SD or n
Age (years)	45 $\pm$ 16
Female	14 (54%)
Obesity	21 (81%)
Diabetes	6 (23%)
Hypertension	3 (12%)
Hyperlipidemia	9 (35%)
BMI (kg/m <sup>2</sup> )	28.4 $\pm$ 4.4
Platelet ( $\times 10^3/\mu\text{L}$ )	245 $\pm$ 70
ALT (IU/L)	85 $\pm$ 59
AST (IU/L)	53 $\pm$ 31
$\gamma$ GT (IU/L)	71 $\pm$ 59
Total cholesterol (mg/dL)	222 $\pm$ 44
Triglycerides (mg/dL)	161 $\pm$ 86
HDL-C (mg/dL)	54 $\pm$ 10
FPG (mg/dL)	109 $\pm$ 23
IRI ( $\mu\text{U}/\text{mL}$ )	18 $\pm$ 12
HbA1c (%)	5.8 $\pm$ 1.0
HOMA-IR	5.2 $\pm$ 4.0
Iron ( $\mu\text{g}/\text{dL}$ )	120 $\pm$ 37
Transferrin saturation (%)	32.8 $\pm$ 12.9
Ferritin (ng/mL)	172 $\pm$ 176

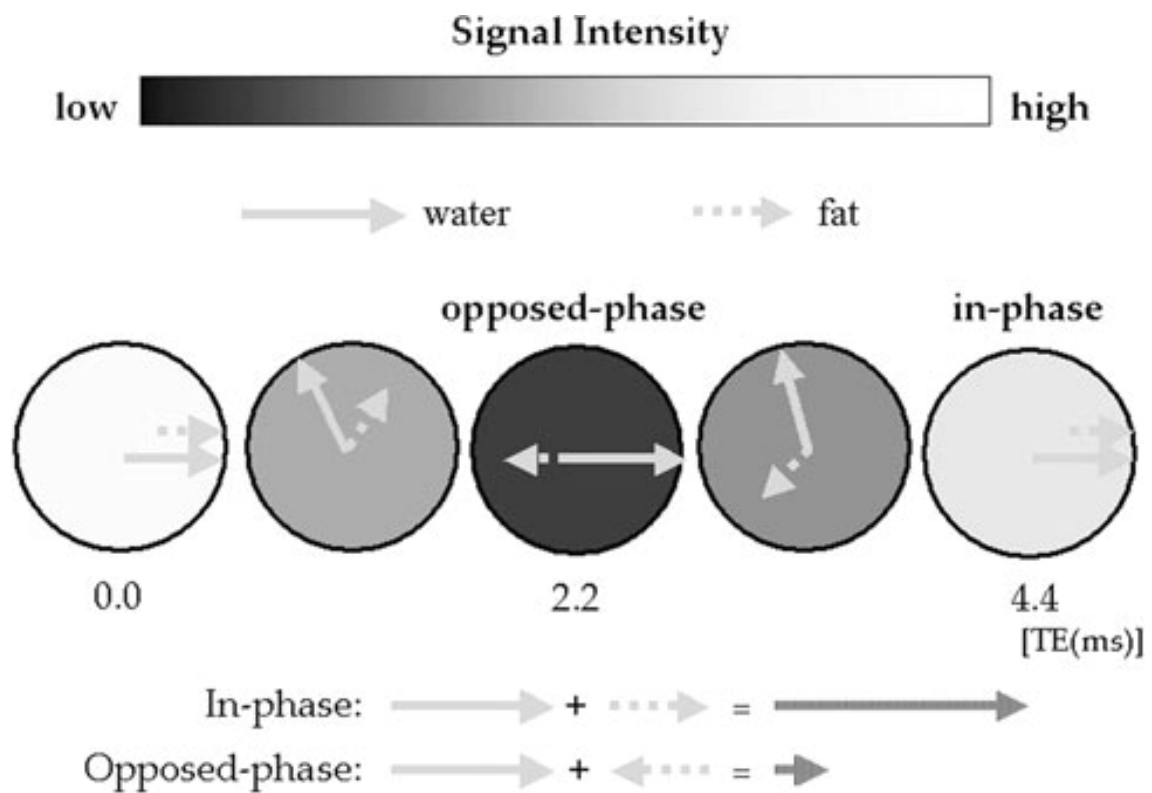
Quantitative data are expressed as means and standard deviation (SD), and qualitative data are expressed as percentages. BMI, body mass index; ALT, alanine aminotransferase; AST, aspartate aminotransferase;  $\gamma$ GT,  $\gamma$ -glutamyltransferase; HDL-C, high-density lipoprotein cholesterol; FPG, fasting plasma glucose; IRI, immunoreactive insulin; HOMA-IR, homeostasis model assessment of insulin resistance.

Table 2. Histological activity and severity, and fat content determined by optical imaging analysis and magnetic resonance imaging (MRI) of the patients

Patient No.	Macrovesicular steatosis	Fibrosis	Lobular Inflammation	Ballooning	NAS	% Fat by optical imaging	% Fat by MR imaging
1	3	1A	2	1	5	38.6	43.2
2	1	1A	1	0	2	15.9	23.2
3	1	1A	1	0	2	16.4	19.2
4	1	1A	1	1	3	20.6	27.0
5	1	1A	1	1	3	25.3	24.2
6	2	1A	2	1	5	24.3	27.6
7	3	1A	3	2	7	32.8	35.4
8	1	2	1	0	1	3.8	5.0
9	3	1A	2	2	7	29.6	34.7
10	2	1A	1	0	3	18.1	22.4
11	2	1A	2	0	4	29.1	29.7
12	2	0	1	0	3	30.2	30.3
13	1	3	2	2	5	9.3	10.3
14	3	0	1	1	5	33.5	36.7
15	1	1A	3	1	5	19.8	21.0
16	1	1A	1	0	2	12.5	14.7
17	2	2	2	2	6	21.2	24.2
18	1	3	2	1	4	6.2	6.7
19	2	1A	2	1	5	20.0	22.0
20	2	0	2	1	5	20.6	27.4
21	3	0	1	1	5	30.7	31.3
22	3	2	3	2	8	27.7	21.2
23	1	0	1	0	2	18.6	9.9
24	2	2	3	1	6	18.3	15.2
25	1	0	1	1	3	14.1	14.8
26	2	0	1	0	3	23.6	18.4

Histological findings were scored according to criteria proposed by Kleiner et al.<sup>5</sup> NAS, nonalcoholic fatty liver disease activity score

## Figure legends



**Fig. 1.**

Schematic diagram demonstrating the principle of chemical shift imaging. With in-phase imaging (TE = 4.4 ms), the water and fat vectors are aligned, and the total signal intensity is additive. In opposed-phase imaging (TE = 2.2 ms), the vectors lie anti-parallel, resulting in partial signal cancellation by vector addition.

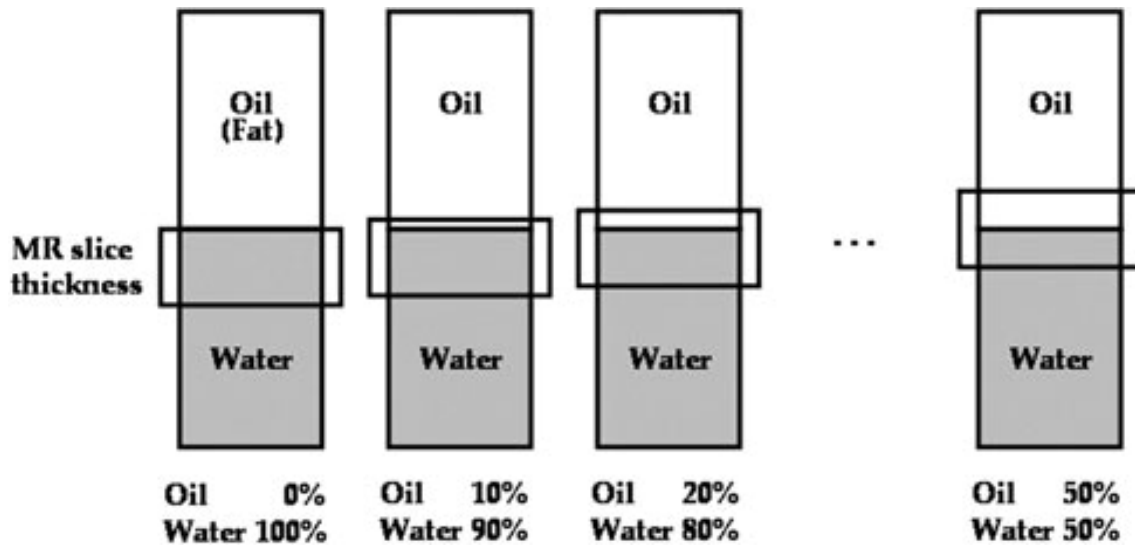


**Fig. 2.**

Schematic presentation of a water-oil phantom. The water-oil phantom using physiologic saline water was layered with mineral oil, which provided a water-oil interface in which to test various fractions of fat to water. Images were obtained in the transverse plane from the bottom (0% oil) to the top (50% oil) of the phantom for various proportions of fat and water protons within each voxel. MR, Magnetic resonance

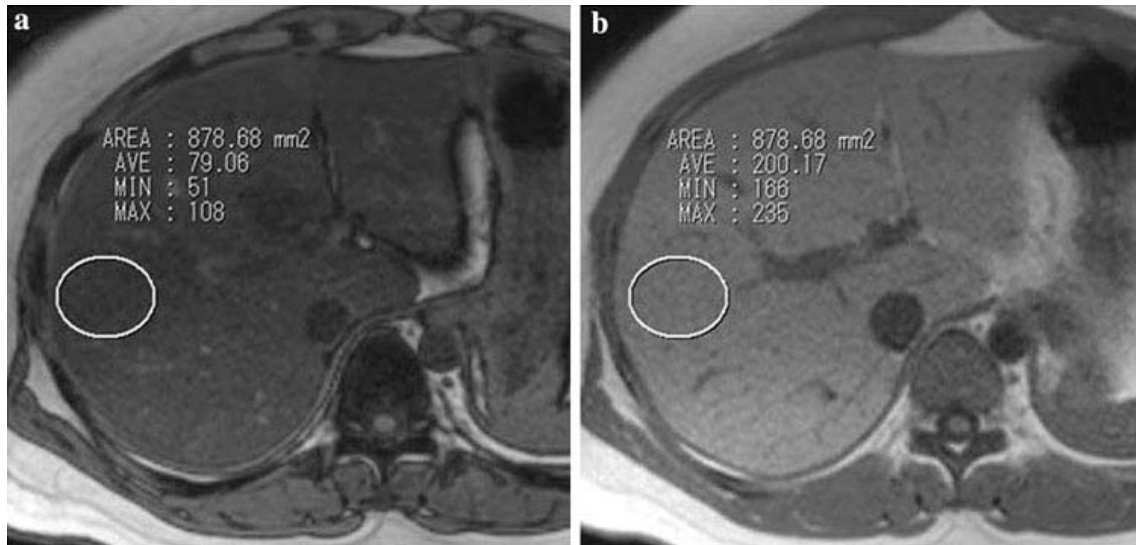


**Fig. 3.**

Quantitation of hepatic fat using magnetic resonance imaging (MRI). MR images of the liver are obtained with (a) opposed-phase and (b) in-phase technique. The regions of interest drawn on each image (circles) measure the mean signal intensities of all cases.

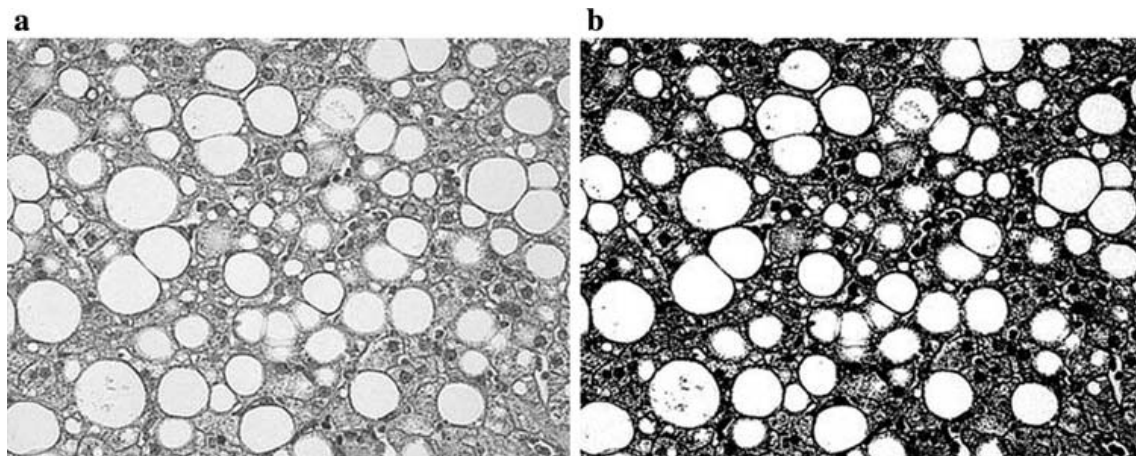


**Fig. 4.**

Digital images of hematoxylin and eosin-stained liver biopsy sections were converted into a gray scale (a), and evaluated to maximize the contrast between fat globules and liver and connective tissue (b).

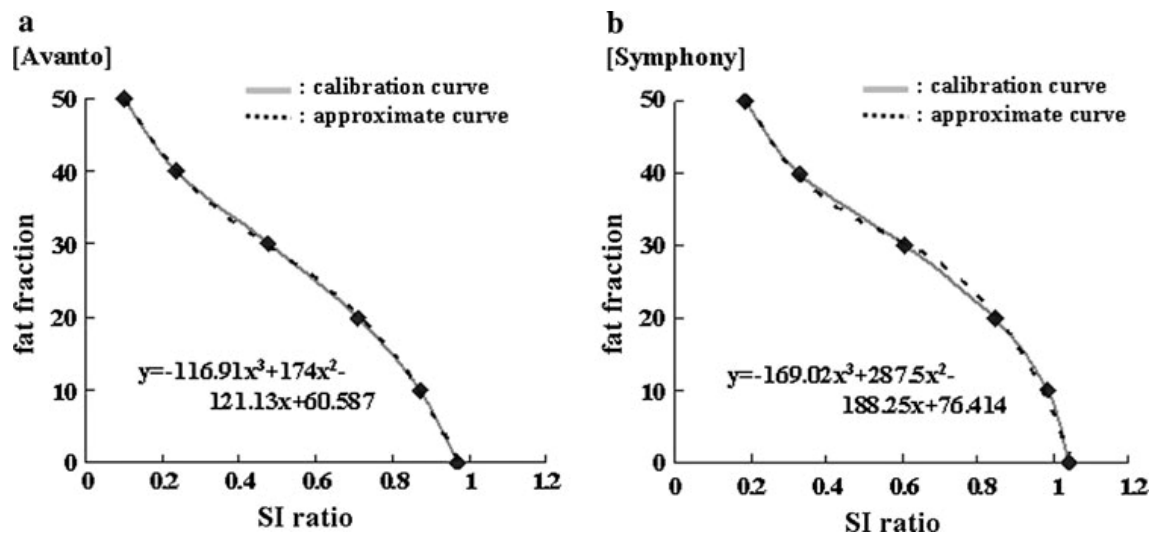


**Fig. 5.**

The fat fraction versus signal intensity (SI) ratio measurements with the phantom and the approximate curve derived from the phantom data ([a: Avanto] and [b: Symphony]).

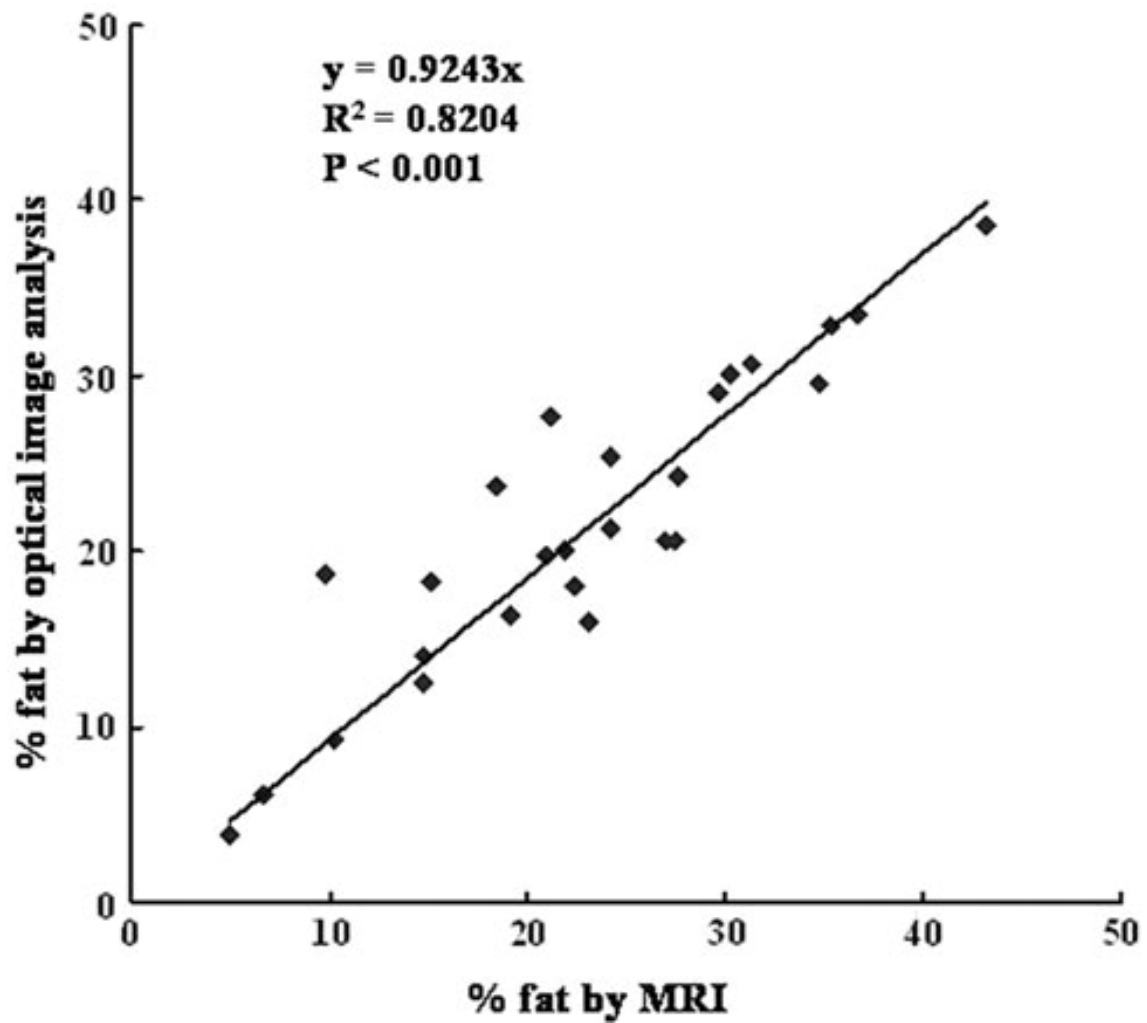


**Fig. 6.**

Relationship between MRI measurements of liver fat content in nonalcoholic fatty liver disease (NAFLD) patients and estimates made by optical image analysis of liver biopsy specimens (n = 26).

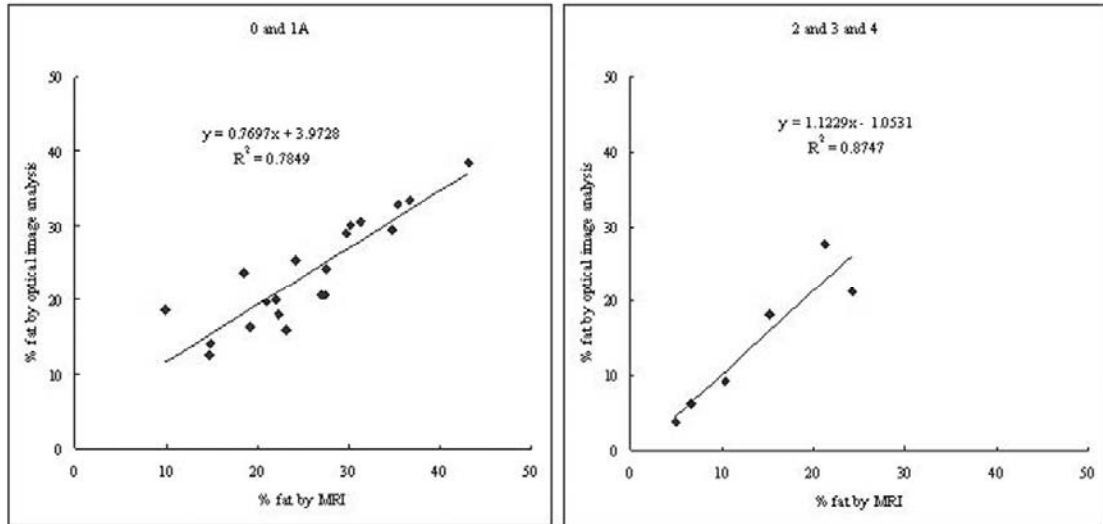


**Fig. 7.**

Relationship between MRI measurements of liver fat content and estimates made by optical image analysis of liver biopsy specimens in patients with (a) significant fibrosis (stage 2-4, n = 6) or (b) not (stage 0 and 1A, n = 20).

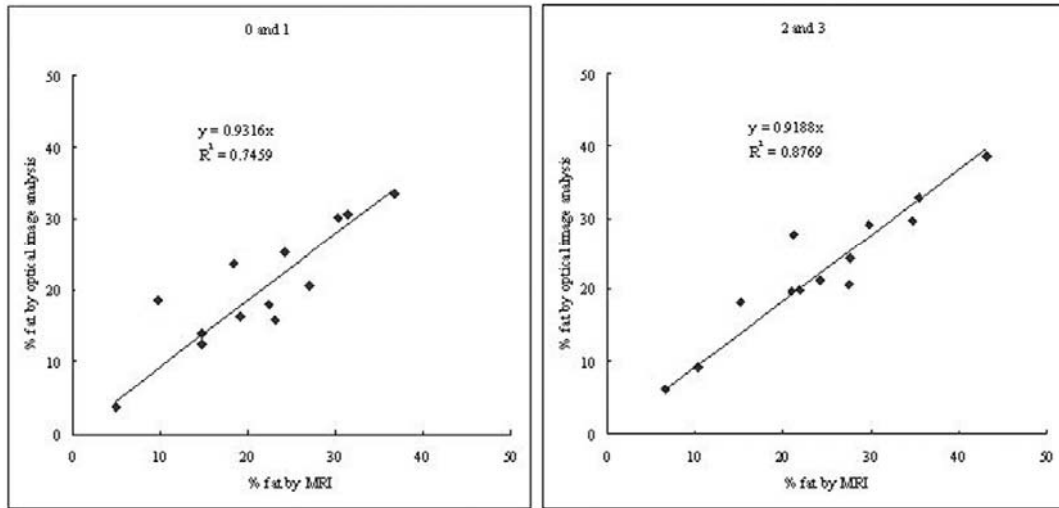


**Fig. 8.**

Relationship between MRI measurements of liver fat content and estimates made by optical image analysis of liver biopsy specimens in patients with lobular inflammation score (a) 0 and 1 (n = 13), (b) 2 and 3 (n = 13).